

# 통합된 PFC 인덕터와 공진변압기의 자기모델링 연구

메아스사란\*, 품쑈피악\*, 김은수\*<sup>†</sup>, 전용석\*, 원종섭\*, 김동희\*\*, 허동영\*\*  
전주대학교\*, LG 이노텍(주)\*\*

## Analysis of an Integrated PFC Inductor and Resonant Transformer Based on Magnetic Modeling

S. Meas\*, S. Phum\*, E.S Kim\*<sup>†</sup>, Y.S Jeon\*, J.S Won \*, D.H Kim \*\*, D.Y Huh \*\*  
Dept. of Electrical Engineering Jeonju University\*, LG-Innotek\*\*

### Abstract

This paper describes the design and analysis of an integrated transformer magnetic core which comprises of two different power cores with PFC inductor and LLC resonant transformer magnetic cores. The equivalent magnetic circuit modeling approach is employed to analyze the variations in coupling coefficient and inductance in terms of air gaps under the operations of the respective power core. Simulation and experimental studies are performed with a fabricated prototype integrated core and their results are discussed.

### Introduction

In recent years, the demand for wide application of highly regulated, reliable power supplies, and the desire to have smaller size, lighter weight and high efficiency of power electronic systems has a big trend. For example, the tallest and heaviest components on printed-circuit-boards are often magnetic components [1,2]. A 2-in-1 transformer core is proposed in this study in order to give one of solutions to cope with the demand. The 2-in-1 transformer core is comprised of a PFC inductor core and an LLC resonant transformer core, which are integrated into one core as shown in Fig. 1.

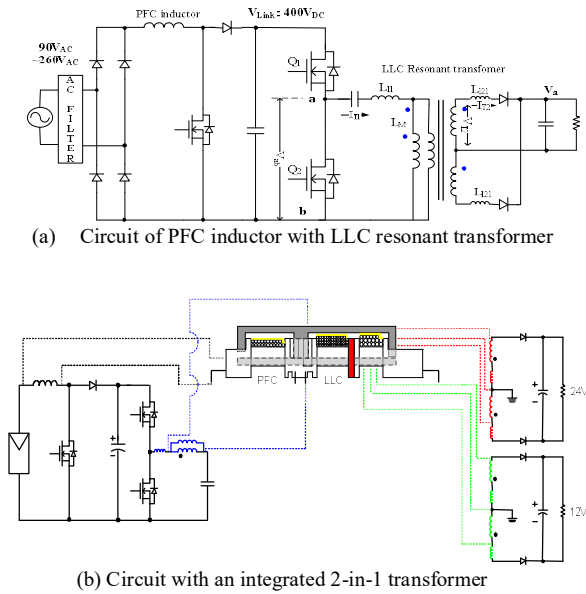


Figure 1. A 2-in-1 transformer proposed in this study

## 2. Transformer Core Structure and Magnetic Circuit Modeling Parameters

### 2.1 Transformer core structure

The proposed core structure that uses only one EI planar core is shown in Fig. 2.

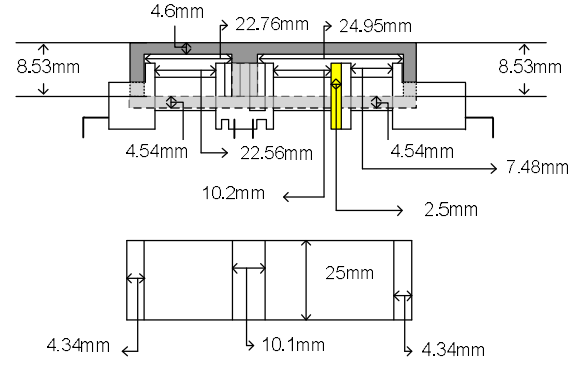


Figure 2. Proposed EI planar core structure

### 2.2 Equivalent magnetic circuit modeling

The proposed magnetic structure is easily modeled as a magnetic circuit as shown in Fig. 3. As described in Fig. 3, reluctance of each part can be calculated by the following equations. It is noted that the reluctance of air gap is larger than that of ferrite cores.

$$\mathfrak{R}_I = \mathfrak{R}_{11} + \mathfrak{R}_{12} + \mathfrak{R}_{13} + \mathfrak{R}_{g1} \approx \mathfrak{R}_{g1} = f_I(l_{g1}; A_{g1}, \mu_0) \quad (1)$$

$$\mathfrak{R}_{II} = \mathfrak{R}_{21} + \mathfrak{R}_{22} + \mathfrak{R}_{23} + \mathfrak{R}_{g2} \approx \mathfrak{R}_{g2} = f_{II}(l_{g2}; A_{g2}, \mu_0) \quad (2)$$

$$\mathfrak{R}_T = \mathfrak{R}_I + \mathfrak{R}_{ig} \approx \mathfrak{R}_{ig} = f_T(l_{ig}; A_{ig}, \mu_0) \quad (3)$$

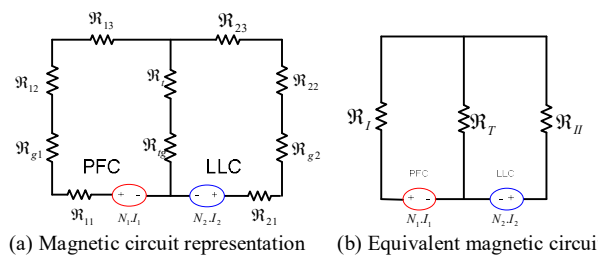


Figure 3. Magnetic circuit modeling of proposed core structure

### 3. Analysis of Transformer Magnetic Circuit Based on Single Operation of PFC Inductor

Under the single operation of the PFC inductor, coupling coefficient and inductance of the integrated 2-in-1 transformer core are calculated based on the magnetic circuit described in Section 2 and their variations in terms of air gaps in the integrated core are discussed.

The analysis in Section 3 and 4 is based on the notion of the superposition theory. For the two power sources in the magnetic circuit described before, by using the superposition theory, the overall behavior of the circuit can be represented by summing the respective behavior from the single operation of each power source. In this section, the PFC inductor is operated as the main power source of the whole transformer core and LLC resonant transformer side is considered as a shorted circuit as shown in Fig. 4.

Theoretic analysis and simulation study (using a commercial program 3D Maxwell) as well as experiments are performed. By using a fabricated prototype core, measurement of inductance is also made.

#### 3.1 Reluctance calculation based on PFC inductor

Given the magneto motive force  $N_1 I_1$  in the PFC inductor, with the approximation in Eqs. (1) through (3), the total reluctance is represented as the function of length and cross-sectional area of each air gap as well as permeability of air.

$$\mathfrak{R}_1 = \mathfrak{R}_I + \frac{\mathfrak{R}_T \times \mathfrak{R}_{II}}{\mathfrak{R}_T + \mathfrak{R}_{II}} = f_1(l_{g1}, l_{g2}, l_{lg}; A_{g1}, A_{g2}, A_{lg}, \mu_0) \quad (4)$$

#### 3.2 Coupling coefficient based on PFC inductor

As the input current is applied to the PFC winding, magnetic flux induced by the current is applied to the whole transformer core. It is expected that the leakage flux through the LLC winding side be small. Thus, in this study, we consider the effect of change in air gap length on the change in the leakage flux. In Fig. 4, notation of magnetic fluxes on the circuit is given and a simulation result from 3D Maxwell using the base values of the prototype core (not listed in the short paper).

The coupling coefficient  $k_1$  is defined as the ratio of leakage flux to main magnetic flux (see Fig. 4 for notation):

$$k_1 = \frac{\phi_{12}}{\phi_1} = \frac{\phi_{12}}{(\phi_{T1} + \phi_{12})} \quad (5)$$

where  $\phi_1 = F_1 / \mathfrak{R}_1$ ,  $F_1 = N_1 I_1$ ,  $\phi_{T1} = (\mathfrak{R}_{eq1} / \mathfrak{R}_T) \times \phi_1$ ,  $\mathfrak{R}_{eq1} = (\mathfrak{R}_T \times \mathfrak{R}_{II}) / (\mathfrak{R}_T + \mathfrak{R}_{II})$ , and  $\phi_{12} = \phi_1 - \phi_{T1}$ .

One can see that the coupling coefficient is also the function of length and cross-sectional area of each air gap as well as permeability of air (refer to Eq. (4)),

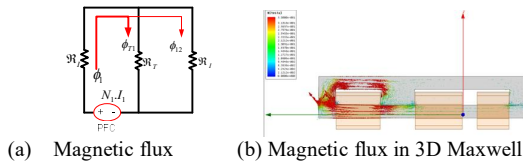


Figure 4. Notation and simulation result based on PFC winding

Figures 5 through 7 show the variation of magnetic flux in Eq.(5) according to the variation of each air gap gap (i.e.,  $l_{g1}$ ,  $l_{g2}$ , and  $l_{lg}$ ). It is observed from Fig. 5 that no variation in  $k_1$  according to the change in  $l_{g1}$  is found for fixed values of  $l_{g2}$  and  $l_{lg}$ . Although the number of flux is varied along with the change in  $l_{g1}$ , the portion of leakage flux at the LLC winding side is not changed and this leads to a constant  $k_1$ . It is noted that the coupling effect

will be disappear when the length of air gap at the center leg's core is zero (see Fig. 6). Furthermore, one can have a small value of  $k_1$  with larger value in length of air gap at the LLC winding side.

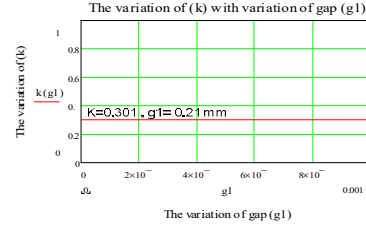


Figure 5.  $k_1$  versus  $l_{g1}$  under a fixed value of  $l_{g2}$  and  $l_{lg}$ .

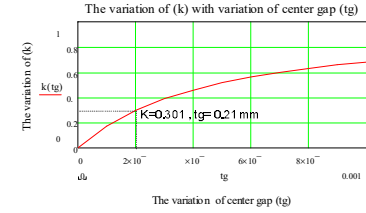


Figure 6.  $k_1$  versus  $l_{lg}$  under a fixed value of  $l_{g1}$  and  $l_{g2}$ .

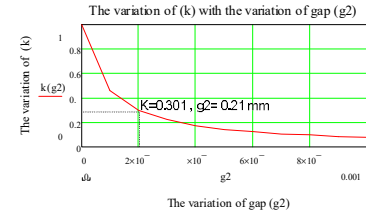


Figure 7.  $k_1$  versus  $l_{g2}$  under a fixed value of  $l_{g1}$  and  $l_{lg}$ .

#### 3.3 Self inductance based on PFC inductor

As the similar manner in the previous section, the variation of self inductance of the integrated core along with the change in respective air gap length has been analyzed. Self inductance is defined as

$$L_1 = \frac{N_1^2}{\mathfrak{R}_1} \quad (6)$$

It is noted that the self inductance is also dependent on the variations of each air gap. The analytic results will be shown in the full paper.

### 4. Analysis of Transformer Magnetic Circuit Based on Single Operation of LLC Resonant Transformer

Under the single operation of the LLC resonant transformer, coupling effect and inductance of the proposed core structure are discussed with the same process in Section 3.

#### 4.1 Reluctance calculation based on LLC transformer

In the presence of the magneto motive force  $N_2 I_2$  in the LLC resonant transformer, the total reluctance of the magnetic circuit is represented as

$$\mathfrak{R}_2 = \mathfrak{R}_{II} + \frac{\mathfrak{R}_T \times \mathfrak{R}_I}{\mathfrak{R}_T + \mathfrak{R}_I} = f_2(l_{g1}, l_{g2}, l_{lg}; A_{g1}, A_{g2}, A_{lg}, \mu_0) \quad (7)$$

#### 4.2 Coupling coefficient based on LLC transformer

Following the same notion in Section 3, coupling coefficient is defined as the ratio of the leakage flux (through the PFC winding) to the main magnetic flux (see Fig. 8 for notation):

$$k_2 = \frac{\phi_{21}}{\phi_2} = \frac{\phi_{21}}{\phi_{T2} + \phi_{21}} \quad (8)$$

Where  $\phi_2 = F_2 / \mathfrak{R}_2$ ,  $F_2 = N_2 I_2$ ,  $\phi_{T1} = (\mathfrak{R}_{eq1} / \mathfrak{R}_T) \times \phi_1$ ,  $\mathfrak{R}_{eq2} = (\mathfrak{R}_T \times \mathfrak{R}_1) / (\mathfrak{R}_T + \mathfrak{R}_1)$  and  $\phi_{21} = \phi_2 - \phi_{T2}$ .

In Fig. 8, notation of magnetic fluxes on the circuit is given and a simulation result from 3D Maxwell using the base values of the prototype core.

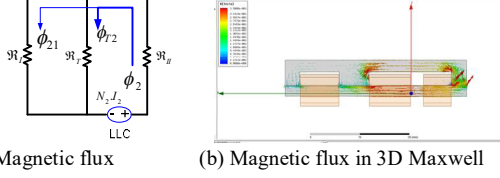


Figure 8. Notation and simulation result based on PFC winding

Figures 9 through 11 show the variation of magnetic flux in Eq.(8) according to the variation of each air gap (i.e.,  $l_{g1}$ ,  $l_{g2}$ , and  $l_{ig}$ ). It is observed from Fig. 9 that the coupling effect is decreased according to the increase in air gap length  $l_{g1}$ . It is noted that the coupling effect will be disappear when the length of air gap at the center leg's core is zero as shown in Fig. 10. It is further noted that no variation in  $k_2$  according to the change in  $l_{g2}$  is found for a fixed values of  $l_{g1}$  and  $l_{ig}$ . Although the number of flux is varied along with the change in  $l_{g2}$ , the portion of leakage flux at the PFC winding side is not changed and this leads to a constant  $k_2$ .

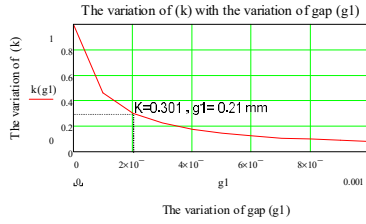


Figure 9.  $k_2$  versus  $l_{g1}$  under a fixed value of  $l_{ig}$  and  $l_{g2}$ .

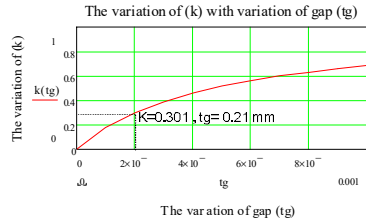


Figure 10.  $k_2$  versus  $l_{ig}$  under a fixed value of  $l_{g1}$  and  $l_{g2}$ .

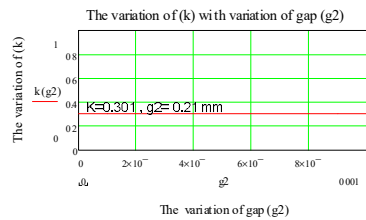


Figure 11.  $k_2$  versus  $l_{g2}$  under a fixed value of  $l_{g1}$  and  $l_{ig}$ .

#### 4.3 Self inductance based on LLC transformer

As a similar fashion in Section 3.3, self inductance is also calculated by using formula in Eq. (9). It is noted that the self inductance is also dependent on the variations of each air gap. The analytic results will be shown in the full paper.

$$L_2 = \frac{N_2^2}{\mathfrak{R}_2} \quad (9)$$

Through Eqs. (5) and (8), coupling coefficient based on the operation of both PFC inductor and LLC resonant transformer can be expressed as follows:

$$k = \sqrt{k_1 k_2} = \sqrt{\frac{\phi_{12}}{\phi_1} \frac{\phi_{21}}{\phi_2}} \quad (10)$$

The coupling coefficient can be obtained by utilizing coupling measurement techniques including a series-aiding and series-opposing methods [3][4]. In the method, coupling coefficient is represented as

$$k = \frac{M}{\sqrt{L_1 L_2}} = \frac{L_{aid} - L_{opp}}{4\sqrt{L_1 L_2}} \quad (11)$$

where  $M = (L_{aid} - L_{opp})/4$ ,  $L_{aid}$  and  $L_{opp}$  are the inductances measured from series-aiding and series-opposing method, respectively.

The values of self-inductance and coupling coefficient of the proposed magnetic structure is given in Table I, which are obtained from different approaches such as analytic, measurement and simulation, under the base values of the magnetic structure in this study.

TABLE I. PARAMETER VALUES OF  $L_1$ ,  $L_2$  AND  $K$

	Obtained from	Value	Unit
$L_1$	magnetic circuit modeling	220.0·10 <sup>-6</sup>	H
$L_1$	measurmt	254.3·10 <sup>-6</sup>	H
$L_1$	Simulation (from 3D Maxwell)	208.8·10 <sup>-6</sup>	H
$L_2$	magnetic circuit modeling	129.8·10 <sup>-3</sup>	H
$L_2$	measurmt	150.3·10 <sup>-3</sup>	H
$L_2$	Simulation (from 3D Maxwell)	130.2·10 <sup>-3</sup>	H
$k$	magnetic circuit modeling	0.301	
$k$	measurmt	0.332	
$k$	Simulation (from 3D Maxwell)	0.343	

### 3. Conclusion

In this paper, an integrated transformer core (2-in-1 transformer), is proposed, which comprised of a PFC inductor and an LLC resonant transformer core. An equivalent magnetic circuit modeling of the proposed core is made and the effects of the change in length of air gaps on the coupling coefficient and inductance have been analyzed depending on the operation of each power source. Theoretical and simulation studies are carried out and measurement of inductance of a prototype core is also made. Analytical and measurement results show the viability of the proposed 2-in-1 transformer core in power supply application.

### ACKNOWLEDGMENT

This work was supported by the cooperative research fund of LG Innotek Co., Ltd.

### Reference

- [1] Pavol Spanik, Ivan Feno, Gabriel Kacsor, "Using Plannar Transformers in soft switching DC/DC Power Converter", University of Zilina, Faculty of Electrical Engineering, Department of Electrical Systems. pp 59-65.
- [2] D.K.W. Chaeng, L.P.Wong, Y.S.Lee, " Modeling, Analysis and Design of Integrated Magnetics for Modern Power Electronics coircuits." IEE 1999 Internation conference on Power Electronics and Dreiver Systems, PEDS. Hong Kong.
- [3] Bryce Hesterman Advanced Energy Industries, "Analysis and Modeling of Magnetic Coupling" Denver Chapter, IEEE Power Electronics Society [www.denverpels.org], pp.1-89.
- [4] S.De Simone, C.Adragna, "Design guideling for magnetic integration in LLC resonant converters", SPEED 2008, International system posium on Power Electronic and Motion. pp. 978-1-4244-1664-6/08.IEEE.